SUPPLEMENTARY MATERIAL

Chemical Recognition of Oxidation-Specific Epitopes in Low Density Lipoproteins by a Nanoparticle based Concept for Trapping, Enrichment and LC-MS/MS Analysis of Oxidative Stress Biomarkers

*Elisabeth Haller,† Gerald Stübiger,[#] Daniel Lafitte,[§] Wolfgang Lindner,† Michael Lämmerhofer‡**

† Department of Analytical Chemistry, University of Vienna, Währingerstrasse 38, 1090 Vienna, Austria

[#] Center of Physiology and Pharmacology, Medical University of Vienna, Schwarzspanierstraße 17, 1090 Vienna, Austria

[§] Faculté de Pharmacie de Marseille, Université de Marseille, 27 Boulevard Jean Moulin, CS 30064 - 13385 Marseille - CEDEX 5, France

‡ Institute of Pharmaceutical Sciences, Pharmaceutical (Bio)Analysis, University of Tübingen, Auf der Morgenstelle 8, 72076 Tübingen, Germany

METHODS AND MATERIALS

Materials. Gold chloride trihydrate ($HAuCl_4 \cdot 3H_2O$), trisodium citrate, ammonium acetate, sodium borohydride, hydroxylamine, cysteamine, methoxyamine, 4-aminobenzoic hydrazide (H_2N-PACa, Amino-PACa) were obtained from Sigma-Aldrich (Vienna, Austria). Plasma was obtained from Technoclone (Vienna, Austria). It constitutes pooled plasma and was obtained from healthy volunteers by informed consent.

Preparation of GNPs. Gold Nanoparticles were synthesized according to the Turkevich-Frens method as described elsewhere.[1] Briefly, 20 mL of 1.28 mM gold chloride trihydrate solution (0.5 mg/mL) were filtered (0.22 µm, Whatman) and heated under constant stirring until boiling. Subsequently, 2.5 mL of a 30.78 mM citrate (9.1 mg/mL) solution was quickly added and the solution kept at ~ 100°C for further 10 minutes. Afterwards, the GNP solution was stirred at RT overnight and characterized by UV-VIS analysis and DLS measurements. The final concentration of gold nanoparticles was 1.64×10^{-6} mM with a size of 28.2 ± 3.1 nm (DLS). The nanoparticle suspension was stored at + 4°C until usage.

UV-VIS. UV-VIS spectra were acquired with a Specord 50 photometer (Analytik Jena, Germany) setting Millipore water as a reference.

Zetasizer. The gold nanoparticles were characterized by analyzing the size distribution by dynamic light scattering and their zeta potential (ζ-potential) by electrophoretic mobility measurements using a Zetasizer Nano ZS instrument (Malvern Zetasizer Instruments Nano

series, Prager Instruments). The refractive index RI was 0.197, absorption 3.90 and water was used as dispersant. The Zetasizer is equipped with a He-Ne laser and detection was performed at 173° backscatter detection mode. Each sample was measured as triplicate and each value was the mean of at least 15 sub-runs.

43 Table S-1 Molecular structures of derivatizing agents and target analytes (PONPC, POVPC).

molecular structure	IUPAC name (supplier)	abbreviation
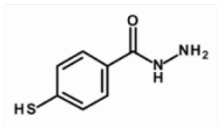	4-Mercaptobenzohydrazide	PACa
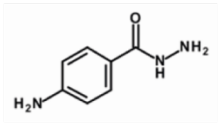	4-Aminobenzohydrazide (Sigma Aldrich, Vienna, Austria)	H_2N-PACa
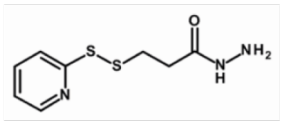	3-(2-Pyridyldithio)propionyl hydrazide (Thermo Fisher Scientific Inc.; Rockford, IL, USA)	PDPH
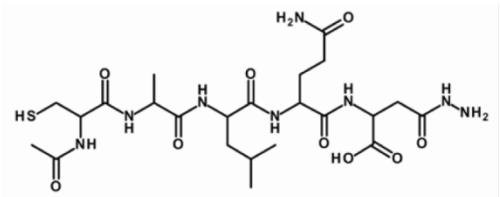	*N*-Acetyl-Cys-Ala-Leu-Gln-Asp-hydrazide (piCHEM, Graz Austria)	CALQD
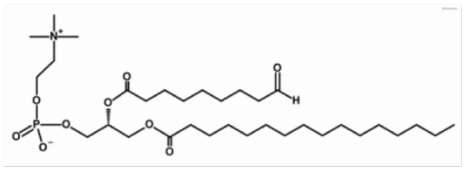	1-Palmitoyl-2-(9'-oxononanoyl)-*sn*-glycero-3-phosphorylcholine (Avanti Polar Lipids, Inc.; Alabaster, AL, USA)	PONPC
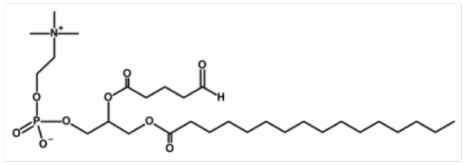	1-Palmitol-2-(5'-oxovaleroyl)-*sn*-glycero-3-phosphorylcholine (Avanti Polar Lipids, Inc.; Alabaster, AL, USA)	POVPC

44

RESULTS AND DISCUSSIONS

Derivatization yields. Fehler! Verweisquelle konnte nicht gefunden werden. of the main document reported the derivatization yields achieved with the distinct (crosslinking) reagents for PONPC. Figure S-1 reveals a comparison of the derivatization yields obtained for PONPC and POVPC in dependence of reagent excess. It can be seen that the results for POVPC are confirming those illustrated for PONPC and the trends are very similar for this different analyte. It can be seen that PACa and H_2N-PACa gave much higher yields than the other two reagents CALQD and PDPH. Among the tested carbonyl trapping reagents, the maximal product yields were observed for PACa (99.0 ± 0.9% and 96.7 ± 2.9% for PONPC and POVPC, respectively) and H_2N-PACa (96.5 ± 3.3% and 97.8 ± 2.1% for PONPC and POVPC, respectively). In contrast, products yields of only 81.5 ± 6.3% (PONPC) and 81.9 ± 2.9% (POVPC) for PDPH and less than 50% for CALQD (46.4 ± 11.7% for PONPC and 47.7 ± 10.3% for POVPC) were obtained.

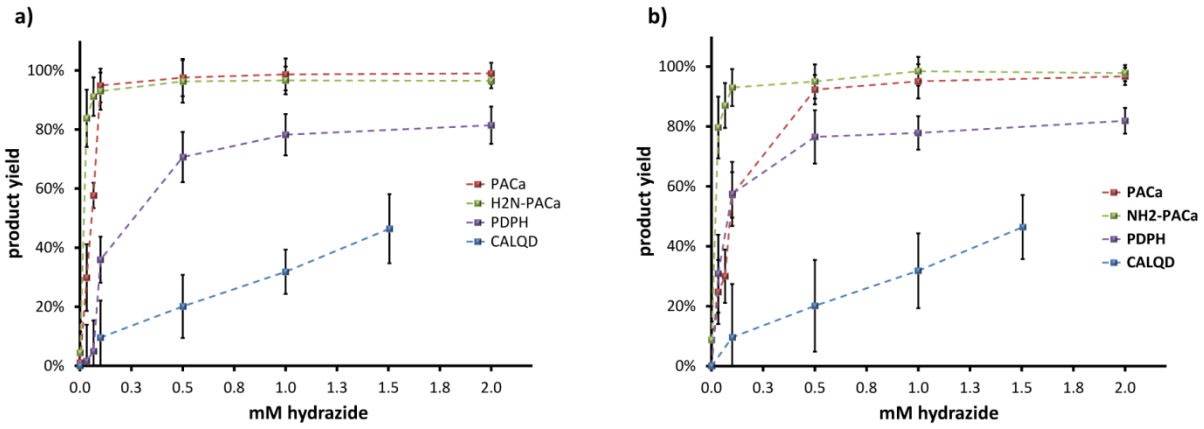

Figure S-1 Reaction yields for a) PONPC and b) POVPC, respectively, with various different derivatizing agents (PACa, H_2N-PACa, PDPH, CALQD).

61 Table S-2 Molecular structures and corresponding abbreviations for the eluted phospholipids.

No.	Molecular structure	abbreviation
(a)	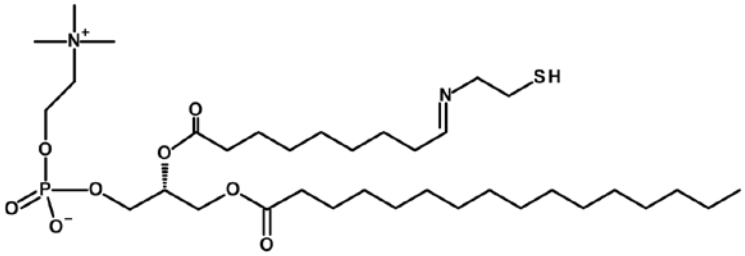	PONPC-cysteamine
(b)	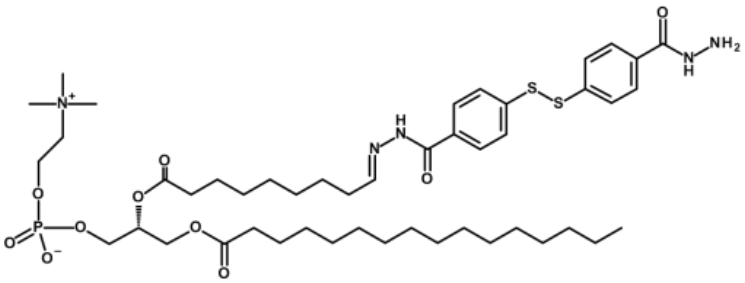	PONPC-$(PACa)_2$
(c)	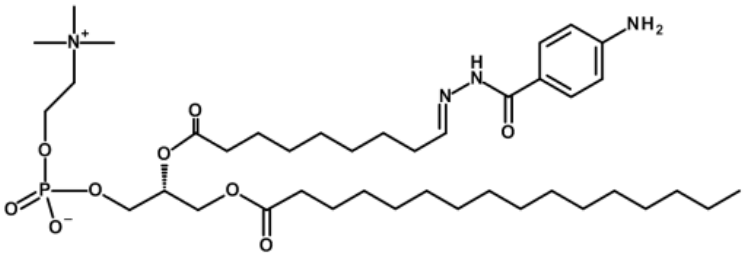	PONPC-PACa–NH_2
(d)	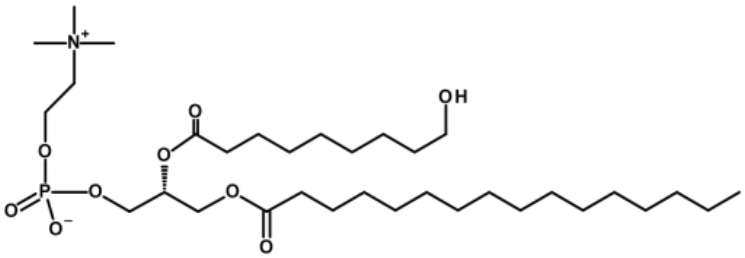	PONPC-OH
(e)	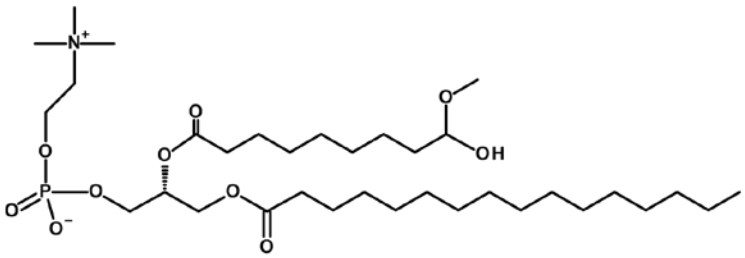	PONPC-hemiacetal

(f)	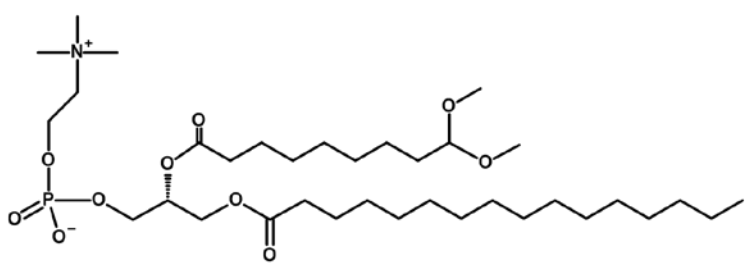	PONPC-acetal
(g)	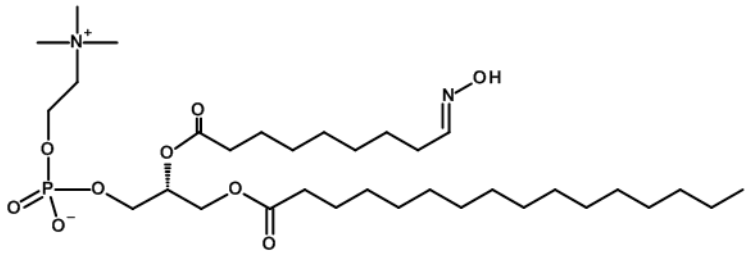	PONPC=NOH
(h)	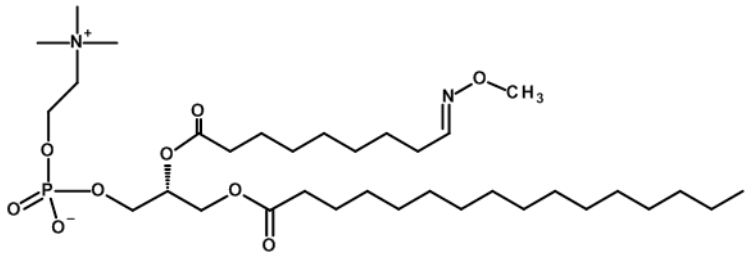	PONPC=$NOCH_3$
(i)	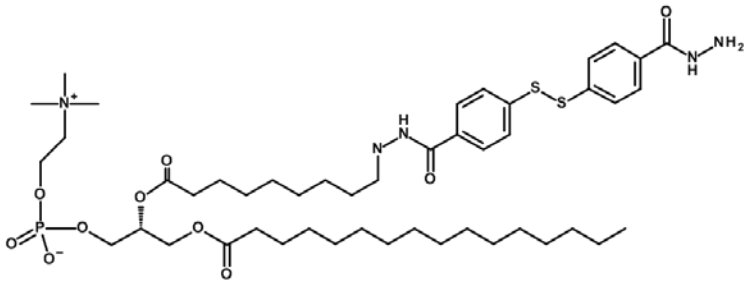	reduced PONPC-$(PACa)_2$

62

63

64

65

66

67

68

69 Table S-3 Parameters for SRM detection of phosphatidylcholines with QTrap 4000 in positive
70 mode.

Molecular species	SRM transition	DP (V)	CE (eV)	CXP (eV)
PONPC	650.5 → 184.1	101	55	14
POVPC	594.4 → 184.1	91	37	10
LPC-16	496.3 → 184.1	116	35	12
LPC-18	524.4 → 184.1	101	39	15
PGPC	610.6 → 184.1	66	41	10
$(PACa)_2$ (dimer)	335.1 → 302.9	41	23	22
H_2N-PACa	152.1 → 94.0	41	19	6
CALQD	605.3 → 330.1	61	25	4
PDPH	230.1 → 143.6	31	15	2
PONPC-$(PACa)_2$ (disulfide)	966.5 → 184.0	106	57	12
POVPC-$(PACa)_2$ (disulfide)	910.4 → 184.1	96	37	10
PONPC-$(PACa)_2$ (disulfide, reduced)	968.6 → 184.1	106	63	12
POVPC-$(PACa)_2$ (disulfide, reduced)	912.4 → 184.1	96	43	10
PONPC-PACa $–NH_2$	783.58 → 184.2	76	53	14
POVPC-PACa $–NH_2$	727.6 → 184.1	91	37	10
PONPC-CALQD	1237.65 → 605.3	66	31	10
POVPC-CALQD	1181.6 → 605.3	66	31	10
PONPC-PDPH	861.5 → 184.1	109	45	6
POVPC-PDPH	805.4 → 184.0	96	37	10
PONPC=NOH	665.5 → 184.2	71	45	12

POVPC=NOH	609.4 → 184.1	91	37	10
PONPC=$NOCH_3$	679.5 → 184.1	91	37	10
POVPC=$NOCH_3$	623.4 → 184.1	91	37	10
PONPC-cysteamine	709.5 → 184.1	106	55	14
POVPC-cysteamine	653.4 → 184.1	96	37	10
PONPC-acetal	696.7 → 184.1	101	55	14
POVPC-acetal	640.6 → 184.1	91	37	10
PONPC-hemiacetal	682.5 → 184.1	101	55	14
POVPC-hemiacetal	626.4 → 184.1	96	37	10
PONPC-OH (red)	652.5 → 184.1	101	45	14
POVPC-OH (red)	596.5 → 184.1	91	37	10

Optimization of release agent and elution conditions. The main document discussed the recoveries for the different releasing agents for both PACa and H_2N-PACa. Depending on release agent, derivatizing agent and employed conditions, the target analytes eluted as distinct derivatives and/or (in minor quantity) as underivatized free target analyte. Below, a more detailed discussion about the profile of eluted compounds and the release efficiency with the distinct agents follows. Table S-2 shows the molecular structures of compounds that have been detected in the course of this study after elution and Table S-3 reveals the corresponding MS-parameters of all ion transitions that have been measured in this study. In the following section, it is partly referred to specific compounds by the code given in Table S-2.

Various agents and strategies for elution of trapped thiol- and amino-terminated oxidized phospholipid-derivatives from the gold nanoparticle surface were examined. PACa and

cysteamine were tested as competitive agents for ligand exchange strategy for analytes trapped *via* Au-S bond and cysteamine, PACa, H_2N-PACa and $NaBH_4$ as competitive agents for ligand exchange for analytes trapped by ionic interactions. Moreover, sodium borohydride is also able to release the thiol by reductive cleavage and formic acid was tested as strategy to reverse hydrazone bond formation under acidic conditions (imines and hydrazones are commonly unstable under acidic conditions). Furthermore, amine containing reagents such as cysteamine, PACa, H_2N-PACa, methoxyamine and hydroxylamine were studied as strategy to release the analytes by transimination.

In order to achieve complete release, high excess of the releasing agents is required which may be problematic for subsequent MS detection. Therefore, the liquid chromatographic separation was coupled post-column with a switching valve which enables time-controlled by-pass of the mass spectrometer when the large excess of the releasing agents eluted from the column (typically with the void or close to it). The results are shown for PONPC trapped *via* thiol-functionalized PACa in Figure S-2 a) and *via* amino-functionalized PACa in Figure S-2 b).

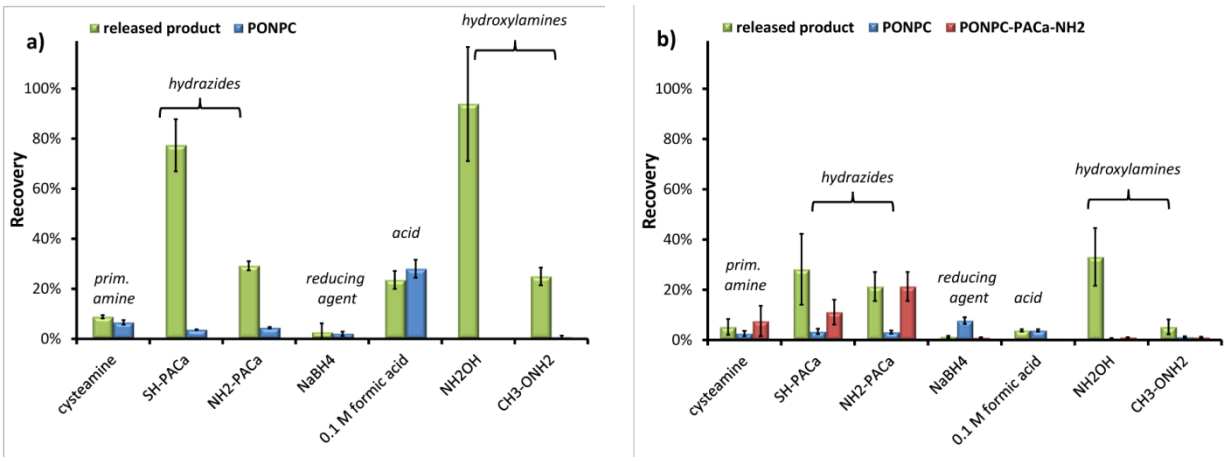

Figure S-2 Comparison of elution strengths of different releasing agents a) of PACa-PONPC-derivative trapped on GNP *via* Au-S bond, and b) for amino-PACa-PONPC derivative trapped on GNPs *via* ionic interactions. The different released products were measured by LC-ESI-MS/MS and are illustrated in Table S-2 (green bars). Besides, also the released PONPC (blue bars) and the released PONPC-PACa-NH_2 (red bars) are depicted in Figure S-2.

In case of addition of cysteamine as releasing agent, analysis of the supernatant revealed that two products were released, namely the corresponding imine formed between PONPC and cysteamine (for molecular structure see Table S-2, compound a) and the PONPC itself. Consequently, it can be concluded that cysteamine is, even in large excess, incapable to competitively displace the bound thiol ligand (PACa-PONPC derivative) from the gold surface. Obviously thiol-thiol ligand exchange is not a good strategy for release owing to the very stable dative thiol-gold bond. Instead, cysteamine with its free primary amino group competes with the hydrazone for carbonyl reaction leading by transimination to the corresponding imine and released analyte derivative, respectively. Unfortunately, the overall yield of release is relatively low (see Figure S-2 a).

For elution with additional PACa, two scenarios are possible: place-exchange reaction of the molecule on the nanoparticle surface by dynamic binding and unbinding processes and transimination. However, in both cases the same product is released (see Table S-2, compound b) and which reaction takes place cannot be distinguished. When using the amino-modified PACa compound (H_2N-PACa) for elution, the competitive imine displacement is the only possible release strategy due to the lower binding affinity of the amino moiety towards gold compared to thiols (see Table S-2, compound c).[2, 3] Comparison of these two hydrazide reagents clearly indicates that the thiol-ligand (PACa) has a stronger competitive effect and release efficiency compared to the H_2N-PACa reagent.

As discussed in the main document, $NaBH_4$ can quantitatively remove thiolates, but re-adsorption takes place. Moreover, sodium borohydride reduces aldehydes and ketones to the corresponding alcohols which would further complicate the situation.[4] Due to re-adsorption processes, analysis of the released phospholipids was performed immediately after addition of $NaBH_4$. Although this procedure enables elution of the bound ligand as PONPC alcohol (see Figure S-2 a), green bars; Table S-2, compound d), the low recovery due to re-adsorption and alcohol formation significantly hampered the subsequent quantitative determination. Besides the PONPC alcohol, also PONPC itself and the non-reduced and reduced PONPC-$(PACa)_2$ (Table S-2; compounds b, i) were released although in a lower extent.

Acidic hydrolysis of the hydrazone bond with formic acid, and thus elution of analyte from the GNPs,[5] was expected to release the original analyte PONPC without any tag (see Figure S-2 a, blue bar). However, various different side-products such as hemi-acetals and acetals (Table S-2, compounds e and f) were observed impeding the subsequent analysis, whereby the green bar in Figure S-2 represents the hemi-acetal (Table S-2, compound e).

Besides, also hydroxylamine and methoxyamine were investigated as releasing agents allowing to elute the analyte by competitive oxime formation *i.e.* transimination. The eluted products are compounds g and h, respectively (see Table S-2). While both release agents afforded a single product, hydroxylamine turned out to be a more efficient releasing agent.

Furthermore, the complete set of releasing experiments was repeated for PONPC bound to GNPs *via* amino-PACa (see Figure S-2 b). The interaction of amino groups with the metal nanoparticle surface is significantly weaker (~ 6 kcal/mol) than that of thiols.[3] Therefore, the H_2N-PACa is weakly bound on the GNP surface due to electrostatic interactions and complex formation, respectively. Further, it has been reported that amines can be easily replaced by thiols present in biological samples.[6] The results for elution efficiency of trapped H_2N-PACa-PONPC were comparable to the PACa crosslinker revealing similar relative elution strengths, but the overall recovery was significantly lower for the trapping strategies with amino-functionalized crosslinker. Thiolated molecules (cysteamine, PACa) exhibit stronger elution strengths due to the higher affinity towards gold releasing the original PONPC-PACa-NH_2 as well as the newly formed hydrazone (red and green bars in Figure S-2 b). However, the presence of more than one released compound makes subsequent quantification complicated.

Calibration, assay performance and application for biological samples. Calibration was performed for both analytes PONPC and POVPC in both standard solutions and plasma by spiking experiments and the summary was already given in Table S-2 of the main document. Figure S-3 depicts the corresponding graphs of the calibration curves for HPLC-ESI-MS/MS analysis without nanoparticle-based enrichment (red symbols) and with enrichment (blue

symbols) (note, a volume reduction factor of 5 was implemented in the case of nanoparticle-based sample preparation). It can be seen that the red curves (without nanoparticle-based sample preparation) are much flatter than the blue curves (with nanoparticle-based sample preparation) which indicates the better assay sensitivity. Linearity data and LOD, LOQ can be found in Table 2 in the main document.

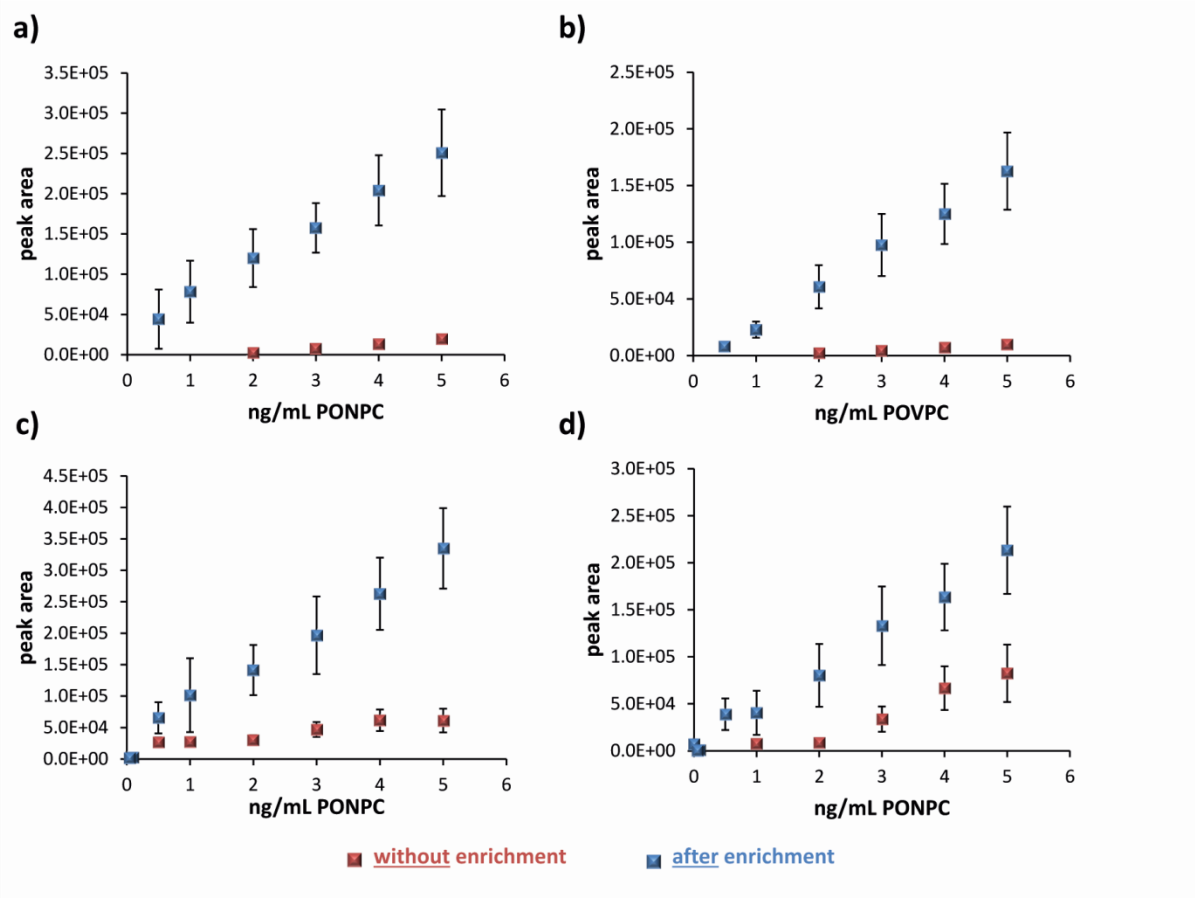

Figure S-3 Comparison of MS signal intensities as measured by peak areas for the aldehydes, PONPC (a, c) and POVPC (b, d), respectively, with and without enrichment employing gold nanoparticles as solid-phase extraction materials. An enrichment factor of 5 was implemented by reducing the volume during the sample preparation. Figure S-3 a) and b) represent the standard solutions and c) and d) correspond to standard solutions spike to plasma.

Solutions with increasing concentrations of MDA-LDL in methanol were analyzed to quantify PONPC and POVPC using the nanoparticle based sample preparation approach in order to determine whether signals increase linearly as expected. Due to limited quantities of MDA-LDL standards the calibration functions were set up only in a very narrow and low concentration range (see Figure S-4, a-c). Comparison with plasma spiked MDA-LDL reveals that the sample extraction procedure gives reasonable recoveries even in complex matrices like plasma. Representative chromatograms are given in Figure S-5.

The same set of experiments was repeated with CuLDL and the results are shown in Figure S-6. It further confirms the applicability of the carbonyl-nanotrap approach for quantitative recovery of carbonylated phospholipids from complex biosamples. Corresponding model chromatograms are given in Figure S-7.

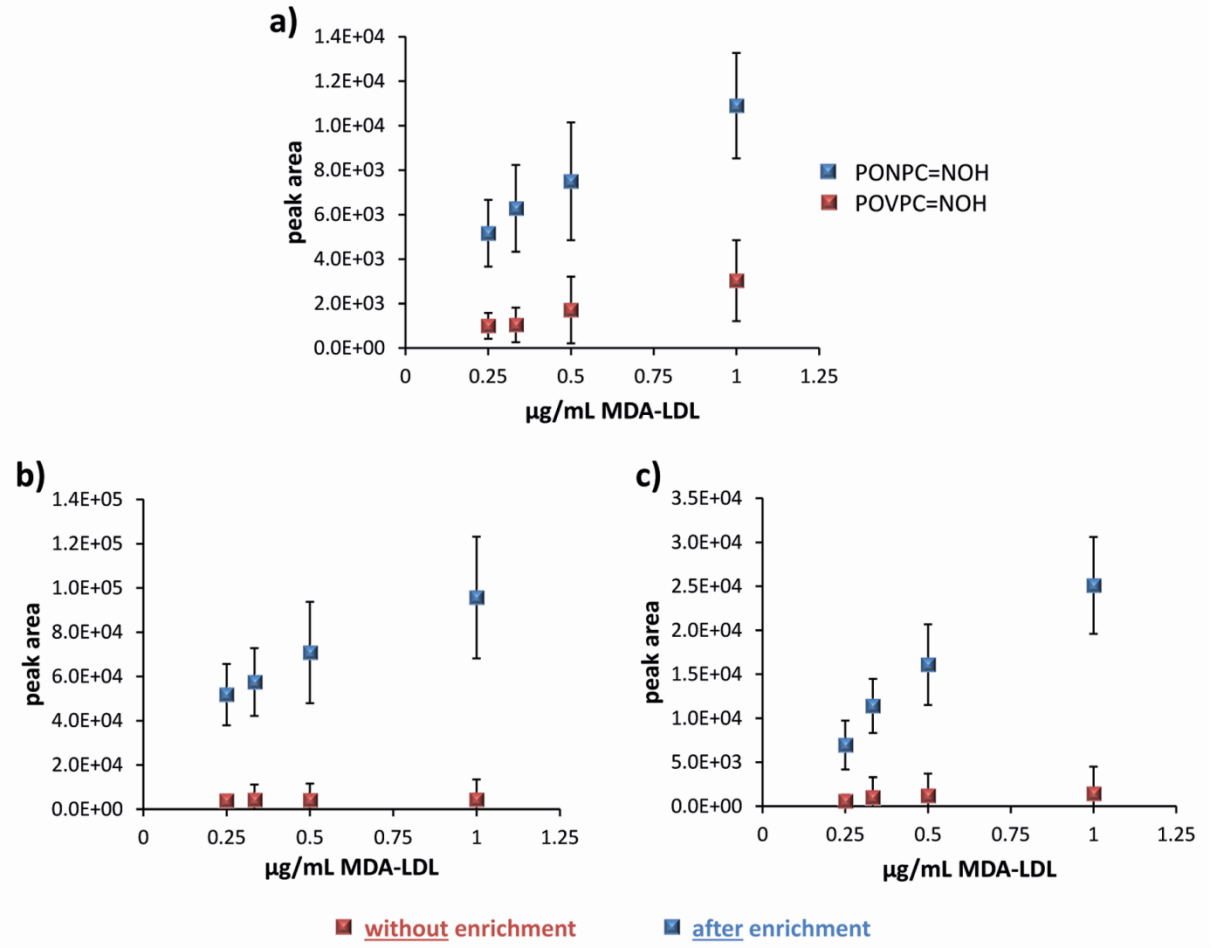

Figure S-4 Extraction of PONPC and POVPC from MDA-LDL (a) and plasma spiked MDA-LDL (b, c) In Figure S-4 a) a final concentration of 0.25 – 1 µg/mL MDA-LDL was extracted using the nanoparticle-based extraction approach. However, performing direct analysis of the same concentrations of MDA-LDL by LC-MS/MS, no signals for PONPC and POVPC, respectively, were detected. In Figure S-4 b) and c) diluted plasma (1:500 in MeOH) was fortified with MDA-LDL with (blue dots) and without extraction (red dots).

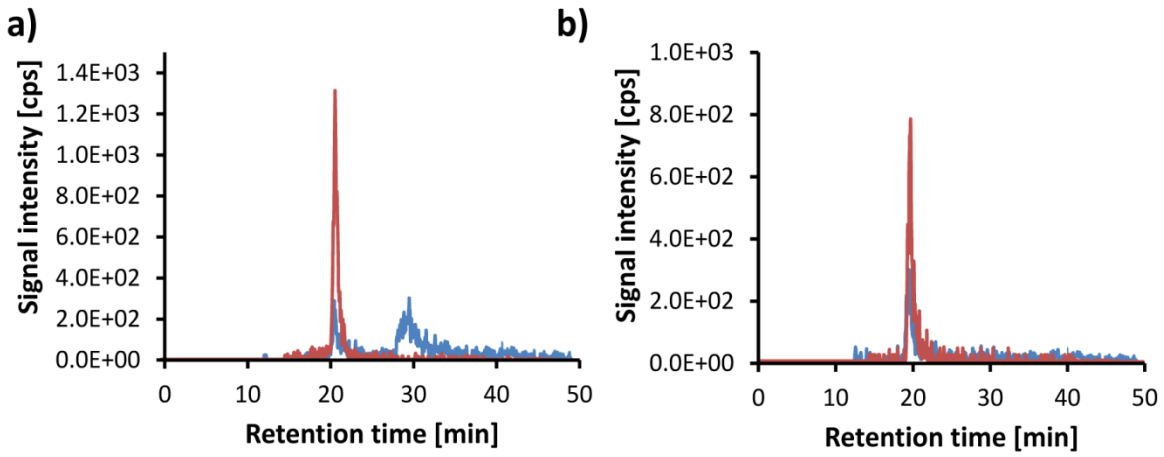

194

195 Figure S-5 MDA-LDL spiked to human plasma (1:500; corresponding to a final concentration of
196 spiked MDA-LDL of 1 µg/ml) a) PONPC and b) POVPC; Blue chromatograms represent the
197 signals analyzed directly after methanolic extraction and the red chromatograms after selective
198 nanoparticle-based extraction.

199

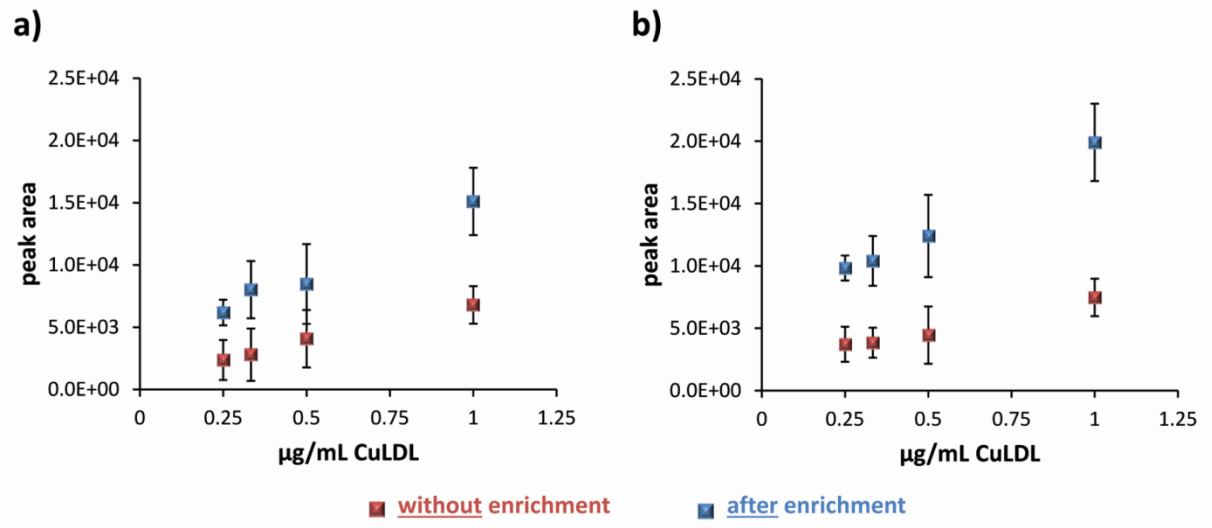

200

201 Figure S-6 Extraction of PONPC from CuLDL (a) and plasma spiked CuLDL (b); note, no
202 POVPC was detected even after enrichment.

203

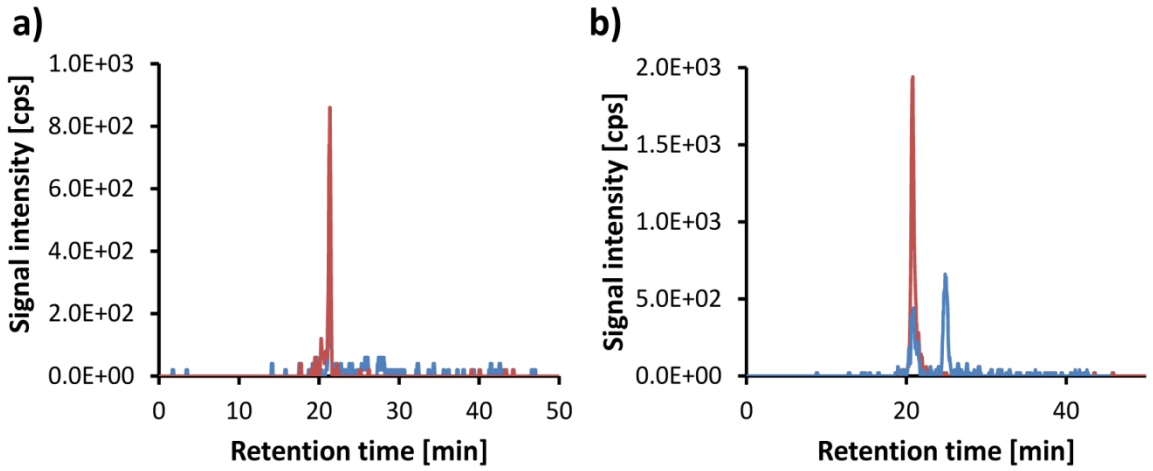

Figure S-7 PONPC in 1 µg/mL of CuLDL was analyzed before (blue chromatograms) and after nanoparticle-based enrichment (red chromatograms). In Figure S-7 a) CuLDL was diluted in methanol, derivatized and extracted by nanoparticles, whereas in b) CuLDL was spiked to human plasma before performing the extraction. In graph b) a second peak with higher retention and the same SRM transition can be seen, illustrating the complex biological matrix. However, after performing the nanoparticle-based extraction only PONPC was enriched whereas the isobaric phospholipid was depleted (red chromatogram).

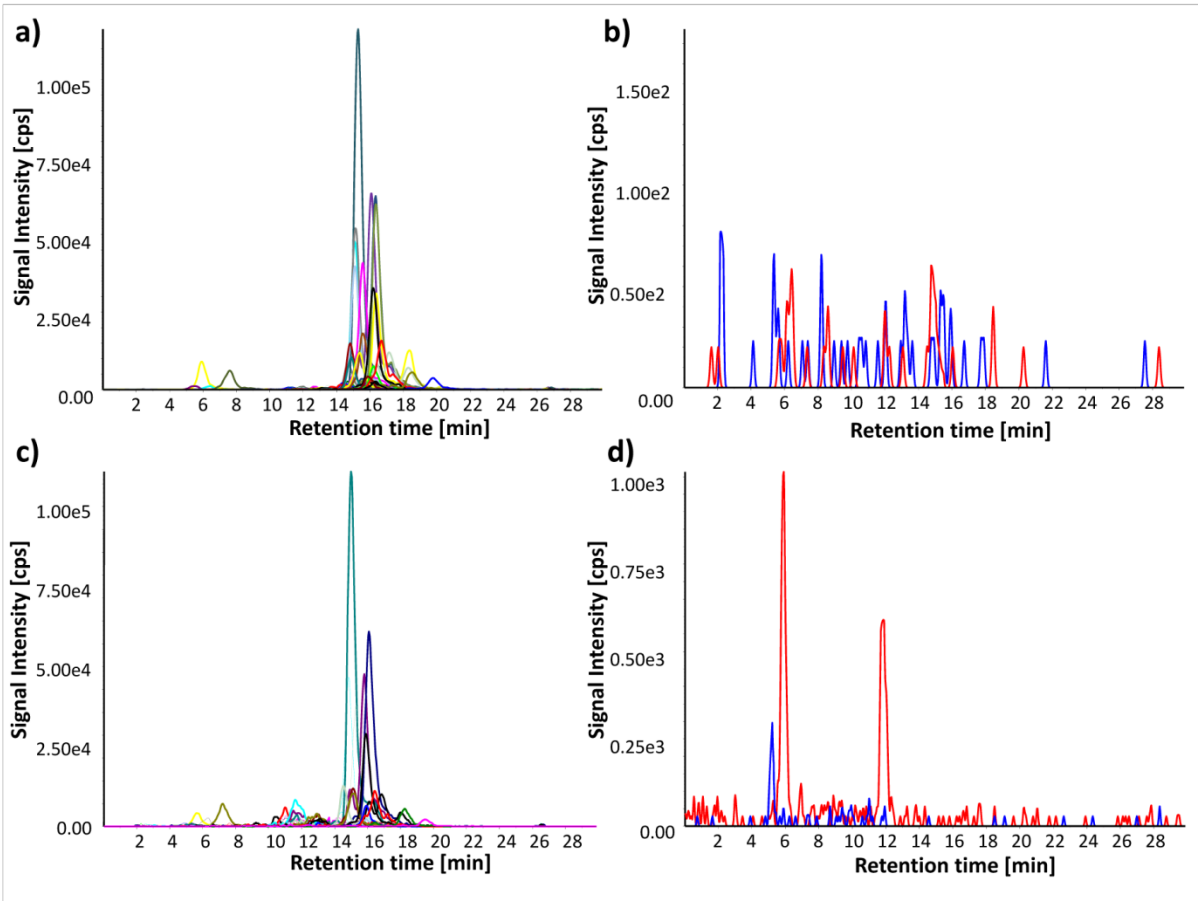

Figure S-8 LC-MS/MS analysis of native LDL (a) and MDA-modified LDL (c) after methanolic extraction. The content of aldehydic compounds, PONPC (red) and POVPC (blue), in natLDL (b) and MDA-LDL (d) is illustrated by their extracted ion chromatograms. In contrast to MDA-LDL, no oxidized phospholipids are present in natLDL (b).

REFERENCES

1. H. Hinterwirth, W. Lindner and M. Lämmerhofer, *Analytica Chimica Acta*, 2012, **733**, 90-97.
2. R. Di Felice and A. Selloni, *The Journal of Chemical Physics*, 2004, **120**, 4906-4914.
3. L. García Fernández, PhD, Universitat Autònoma de Barcelona, 2013.
4. A. D. Watson, N. Leitinger, M. Navab, K. F. Faull, S. Hörkkö, J. L. Witztum, W. Palinski, D. Schwenke, R. G. Salomon, W. Sha, G. Subbanagounder, A. M. Fogelman and J. A. Berliner, *Journal of Biological Chemistry*, 1997, **272**, 13597-13607.
5. J. Kalia and R. T. Raines, *Angewandte Chemie International Edition*, 2008, **47**, 7523-7526.
6. M.-A. Neouze and U. Schubert, *Monatshefte für Chemie / Chemical Monthly*, 2008, **139**, 183-195.